Purdue University
Purdue e-Pubs

International Refrigeration and Air Conditioning Conference

School of Mechanical Engineering

2018

Modeling of Acoustics Based Geometry Optimization of Orifice Tube Design

Yingyue Zhang
UIUC, United States of America, yingyue2@illinois.edu

Stefan Elbel
elbel@illinois.edu

Follow this and additional works at: https://docs.lib.purdue.edu/iracc

Zhang, Yingyue and Elbel, Stefan, "Modeling of Acoustics Based Geometry Optimization of Orifice Tube Design" (2018). *International Refrigeration and Air Conditioning Conference.* Paper 1863.
https://docs.lib.purdue.edu/iracc/1863

This document has been made available through Purdue e-Pubs, a service of the Purdue University Libraries. Please contact epubs@purdue.edu for additional information.
Complete proceedings may be acquired in print and on CD-ROM directly from the Ray W. Herrick Laboratories at https://engineering.purdue.edu/Herrick/Events/orderlit.html

Modeling of Acoustics Based Geometry Optimization of Orifice Tube Design

Yingyue Zhang[(a)], Stefan Elbel [(a, b*)]

[(a)] Air Conditioning and Refrigeration Center,
Department of Mechanical Science and Engineering,
University of Illinois at Urbana-Champaign,
1206 West Green Street, Urbana, IL 61801, USA
[(b)] Creative Thermal Solutions, Inc.,
2209 North Willow Road, Urbana, IL 61802, USA
[(*)] Corresponding Author
Email: elbel@illinois.edu

ABSTRACT

Flow-induced noise in expansion devices is always a severe problem in HVAC&R applications, such as the TXV noise in an automobile where users are sensitive to noise emissions. This paper introduces a CFD based model for exploring the geometry optimization of an orifice tube using R134a. Relevant parameters including diameter and internal geometry features are discussed in the paper. When the flow is going through the constrained section, liquid R134a turns into vapor. In this paper, the internal fluid flow is solved separately as large eddies and small scales with 3D large eddy method. Phase change that happens in the orifice is computed using mass transfer between liquid R134a and vapor R134a that is similar to what happens in cavitation. The cavitation model is used together with a simplified multiphase model – mixture model. The fluid model and structure model interact with each other with two interactive surfaces within each solving step. Natural frequency describes the vibration of the orifice tube when the interior flow is going through, while vortex shedding frequency is generated when internal flow hits bluff geometry features. The modification of internal geometry significantly mitigates the flow-induced noise by reducing the turbulence of flow field. Increasing the tube wall thickness also weakens the flow-induced noise by lowering resonance with structure vibration. The results are references for geometry optimizations of other types of expansion devices, such as manual expansion valve and TXV.

1. INTRODUCTION

Refrigerant-induced noise is a combination of fluid-acoustic and structure-acoustic phenomena (Gijrath and Ăbom, 2003). Flow-Induced noise caused by expansion devices is in the frequency range of thousands of Hertz. The flow oscillations after being throttled by the expansion devices are transmitted as plane waves, some of which formulate higher order acoustic modes within the tube. These acoustic modes could be propagated when coupling with tube wall. The natural frequency of the circular tube determines the structural modes of orifice tube. The flow oscillations including vortex shedding, collision with the tube wall and possible flashing flow are the sources of flow-induced noise. Gurgling noise and hissing noise are the two main types of flow-induced noise. A gurgling noise distributes between 4-7 kHz while a hissing noise distributes over 10 kHz. Flow-induced noise in the automobiles can be very disturbing, so that is always of great concern. Noise mitigation is often done after the design is completed and fixing the problem afterward can be very costly. It is beneficial to establish a model that can simulate the acoustic characteristics of fluid flow and structure together in the expansion devices. The modeling results can provide suggestions for geometry improvements before manufacturing.

The orifice tube is one of the most common expansion devices and is used in this paper for optimization. In this paper, natural frequency and vortex shedding frequency are introduced as important parameters that influence the flow-induced noise. The paper employs ANSYS software for modeling the performance of the tube wall and the flow field. Fluent-Structure Interaction (FSI) model is applied to simulate how fluid flow and structure body interact with each other in inducing noise. By comparing the modeling results based on the orifice tube with different internal geometries and tube wall thickness, the paper illustrates the relationship between geometry differences and flow-induced noise.

2. THEORY OF COMPUTATIONAL METHOD

2.1 Vortex Shedding Frequency and Natural Frequency

When the geometry is disturbed, the geometry vibrates at the excitation's frequency at descending amplitude. When the excitation's frequency reaches natural frequency, the geometry will vibrate at a certain frequency without energy attenuation. The certain frequency is called natural frequency. Eight structural modes are defined in Figure 1, the natural frequency of each mode is determined accordingly in equation (1) and equation (2) (Blevins, 1979):

$$f_{m,n} = \frac{\lambda_{m,n}}{2\pi a_{mi}} \left[\frac{E}{\rho_{ma}(1-\nu^2)} \right]^{\frac{1}{2}} \tag{1}$$

$$\lambda_{m,n} = \frac{\left\{ (1-\nu^2)\left(\frac{m\pi a_{mi}}{l}\right)^4 + \left(\frac{h^2}{12(a_{mi})^2}\right)\left(n^2 + \left(\frac{m\pi a_{mi}}{l}\right)^2\right)^4 \right\}^{\frac{1}{2}}}{n^2 + \left(\frac{m\pi a_{mi}}{l}\right)^2} \tag{2}$$

Aluminum tube starts vibrating at about 6.7 kHz (internal diameter 12 mm, 0.13m length, 1mm thickness). The second order of structure vibration starts at 13 kHz. Flow oscillations including vortices, flashing flow and random collisions with the tube wall formulate several acoustic modes within the orifice tube. The flow regimes after being throttled are so complicated that the speeds of fluid flow vibrations are hard to estimate. Vortices usually appear after the flow hitting the bluff body. Similarly, when the refrigerant flow hits the internal bluff structure of the orifice tube, the vortices appear at the corner. The inflow velocity before the bluff body determines vortex shedding frequency. Meanwhile, the equivalent diameter (B) of the bluff is the radius of the constrained section. Based on numerical and experimental results (Valipour *et al.*, 2008), the Strouhal number (*St*) is 0.22 (as shown in Figure 2), the vortex shedding frequency (*f*) is determined by equation (3):

$$f = St\frac{V}{B} \tag{3}$$

When the natural frequency and the flow oscillation frequency match, flow-induced noise is amplified. The lock-in relationship between flow and structure exists within a certain range as shown in equation (4):

$$0.8f_{m,n} < f < 1.2f_{m,n} \tag{4}$$

The resonance of structure and flow usually increases the flow induce noise volume by 3 dB (Blevins and Bressler, 1993).

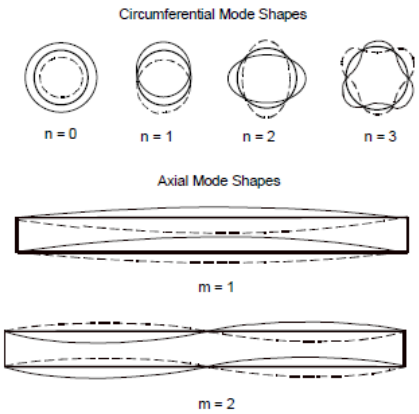

Figure 1: Structural modes (Rodarte *et al.*, 1999)

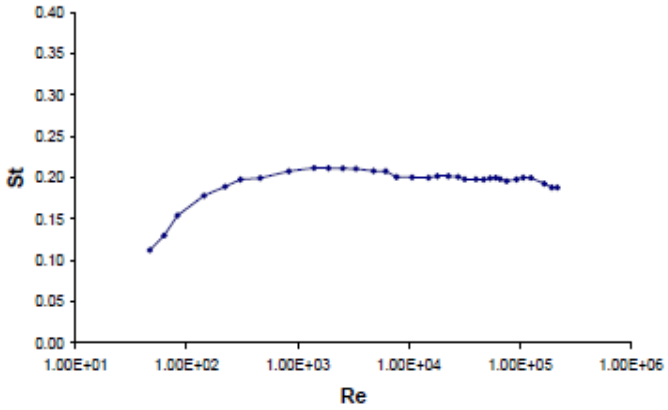

Figure 2: Strouhal number v.s. Reynold number (Valipour *et al.*, 2008)

2.2 Fluid Model

Large eddy simulation (LES) turbulence model used in jet noise prediction simulation, saves computational cost by ignoring the smallest length scale. The small-scale physical process cannot be accurately solved by the computational mesh so that subgrid-scale modeling is used to resolve small-scale fluid motions. Small-scale turbulence is modeled using a Smagorinsky model with Lilly's modification. The Ffowcs Williams-Hawkings (FWH) solver post-processes the existing LES database for acoustic results (Mendez *et al.*, 2013).

LES method and U-RANS method are compared in solving vortex and acoustic emissions in rod-airfoil modeling (Jacob *et al.*, 2005). By seeding the air flowing to the rod-airfoil, air velocity distribution is observed based on captured pictures (PIV). Regarding velocity distribution, microphones are placed in different positions for recording noise. Figure 3 shows LES computational results are closer to the real acoustic distribution when the flow is passing the rod-airfoil.

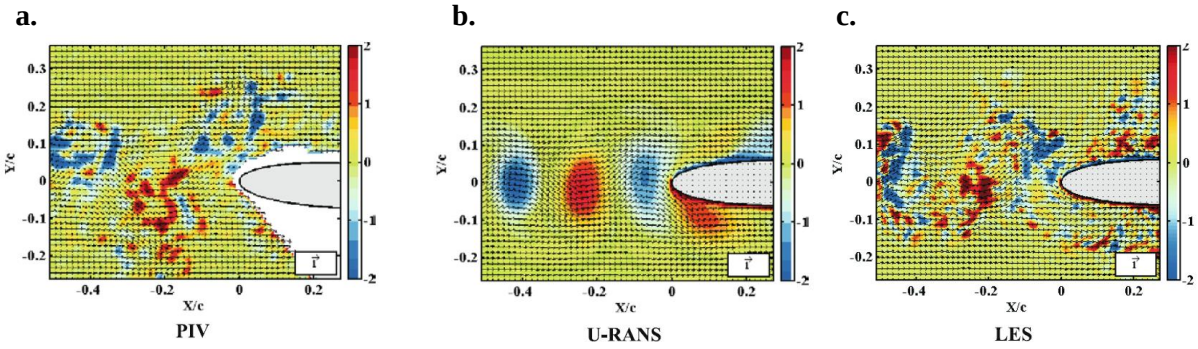

Figure 3: The acoustic modeling results (Fig 3b shows the modeling results of U-RANS method and Fig 3c shows the modeling results of LES method) and experimental results comparison (Fig 3a) (Jacob *et al.*, 2005)

In this paper, mass transfer between the liquid phase and vapor phase happens inside the orifice tube. When the flow is going through the orifice tube's constrained part, local static pressure decreases, and local average flow velocity increases. When the static pressure inside the orifice tube drops to lower pressure than the saturation pressure, the phase change occurs. Therefore, the homogeneous multiphase flow going through the orifice tube is computed in this paper by cavitation model. No bubbles are created and destroyed during the phase change process so that the bubble number density is constant. The surface tension of between R134a vapor and R134a liquid is set to 7.58 mN/m (Chae *et al.*, 1990). The vapor pressure is 550 kPa, assuming the same during throttling process. Since the Mach number for this case is smaller than 0.3, the fluid flow is considered as an incompressible flow.

2.3 Coupling Model

Flow-induced noise heard by people is the coupling effect of the flow oscillation and the tube wall propagation. The paper uses coupling model to solve the interaction between the orifice tube wall and the fluid flow. The physical quantities between two interactive boundaries are the core solving step in coupling system (Lotfi *et al.*, 2016). The detailed solving process of FSI model is shown in Figure 4. Within each time step, the fluid model takes the boundary data from structure model and vice versa. In this paper, the interface is the contact surface between inner structure wall and fluid flow.

The geometries of different orifice tubes are shown in Figure 5. The orifice tube is made up of aluminum. In the axial direction, elastic support is applied to the boundary cross-section. No displacement is allowed in the other two directions at the boundary. The shape of bearing surface is a circular ring for this case so that the foundation stiffness (K) is determined based on equations (5) and (6):

$$K = \frac{3EI}{D^3} \tag{5}$$

$$I = \frac{1}{12} l^3 (D\text{-}d) \tag{6}$$

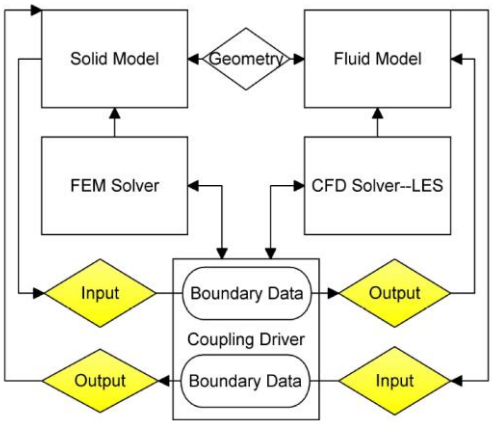

Figure 4: Coupling system layout

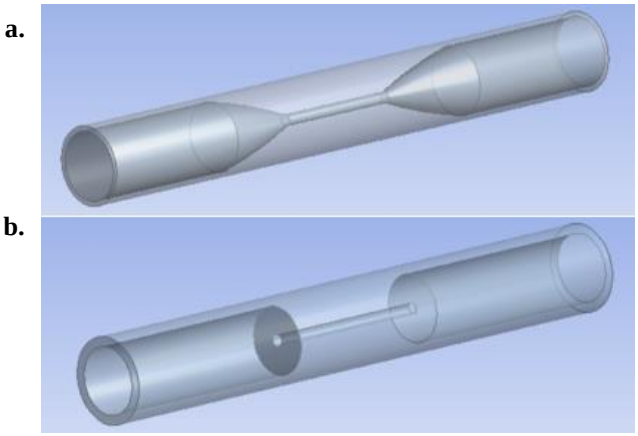

Figure 5: Different orifice tube geometries (Fig 5a for the diverging orfice tube with 1mm-thickness tube wall, Fig 5b for the parallel orifice tube with 2mm-thickness tube wall)

2.4 Meshing Quality and Quantity

The quality of the mesh plays a significant role in the accuracy and stability of the numerical computation. In this case, the mesh type is quadratic whose maximum length scale is 1mm. Refinement is used on the edges. The worst cells will have an orthogonal quality closer to 0, and the best cells will have an orthogonal quality closer to 1. Figure 6 shows the mesh quality of the structure model and the fluent model. The number of elements for each case is displayed in Table 1.

Table 1: Number of elements of different models for different cases

	Number of elements of the fluid model	Number of elements of the structure model
Diverging orifice tube (1 mm-thickness)	68195	43535
Parallel orifice tube (1 mm-thickness)	86416	40848
Parallel orifice tube (2mm-thickness)	87547	56488

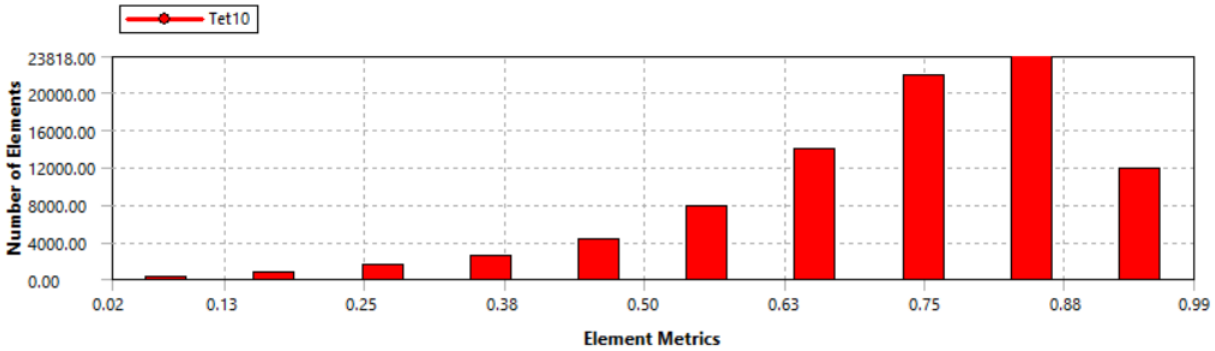

Figure 6: Orthogonal quality for meshing for the FSI model (same quality for the fluid model and structure model)

3. RESULTS AND DISCUSSIONS

3.1 Initialization

The boundary conditions are set up based on measurements obtained from a real R134a refrigeration system. The inlet flow is the R134a flow with 9.8 ℃ subcooling, so the volume fraction of vapor phase is zero. The length of the constrained section for expanding the flow is determined based on the inlet and outlet flow conditions. The inlet velocity of R134a flow is about 0.5m/s at 65g/s, a typical mass flow value in the R134a refrigeration cycle. The outlet pressure, in this case, is 550 kPa.

3.2 The Acoustic Modelling Results of Orifice Tube with Different Internal Geometry

Two orifice tubes share the same tube wall thickness with different internal geometries. Apparent vortices appear in the corner after being throttled by the constrained section in the parallel orifice tube, while only a few vortices appear in the other design, a diverging orifice tube. The vibration amplitude of the tube wall is determined by the total acoustic energy transmitted to the structure. The equivalent sound pressure level is calculated by the acoustic energy transmitted to the surface. In Figure 7 and 9, the amplitudes of the parallel orifice tube vibration and the diverging orifice tube vibration are compared. The orifice tubes in the two cases have very small deformation of tube wall when the fluid flow is going through. It is the flow oscillations after being throttled by a constrained section that causes severe vibrations of the orifice tube (the structural modes of vibration refer to Figure 1). Vortices in the parallel orifice tube excite the tube wall into more severe vibration than the diverging orifice tube design. The velocity distributions of flow inside parallel orifice tube and diverging orifice tube are shown in Figure 8 and Figure 10. The vortex shedding frequency is about 3 kHz to 4 kHz in this case, so that noise generated by vortices will not vibrate in resonance with the tube structure.

In this model, a sound receiver is located 5cm away from the orifice tube wall. The spectra of the two cases are compared in Figure 11; the flow-induced noise is mitigated throughout the frequency domain. As the lock-in phenomenon mentioned in the literature occurs, flow oscillations vibrating at between 5.4 kHz to 8 kHz can couple with the first order structural mode of the tube and reach resonance together. Besides, flow oscillations vibrating at between 10.4 kHz to 15.7 kHz can couple with the second order structural mode of the tube. The modeling results match the literature very well for the parallel orifice tube. The noise induced by vortices (3 kHz to 4 kHz) at the corner decrease by 6 dB. The sound that vibrates at above 9 kHz in the diverging orifice tube is weakened by almost 10 dB. That is because the diverging geometry reduces the turbulence of the outlet flow. The decrease in the number and strength of vortices and also fewer flow-structure collisions weaken the flow-induced noise.

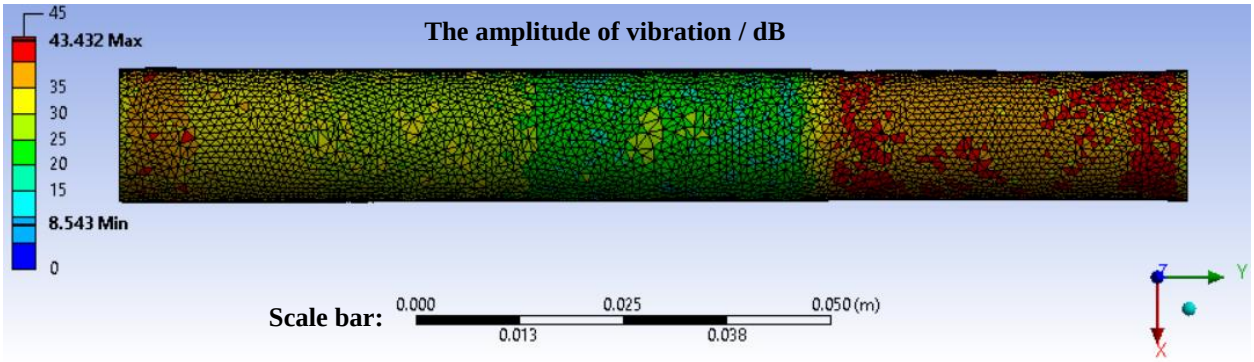

Figure 7: Equivalent sound pressure level (dB) of the parallel orifice tube.

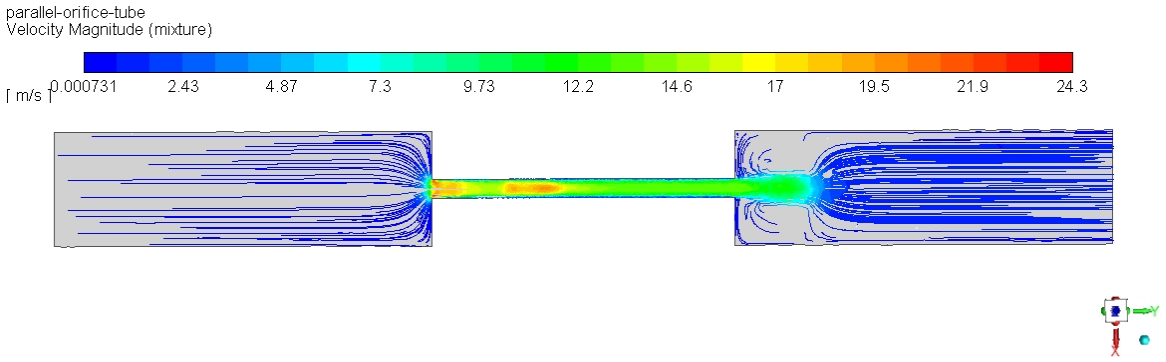

Figure 8: Velocity distribution of flow inside the parallel orifice tube

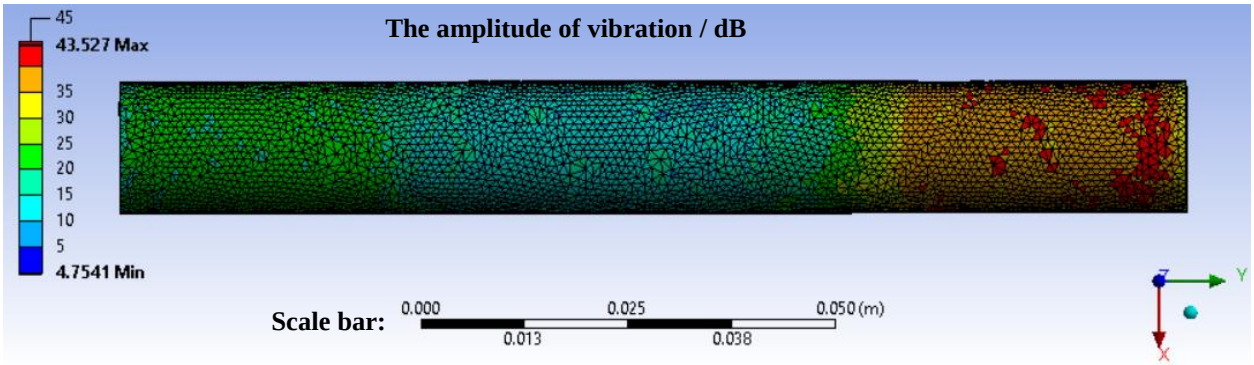

Figure 9: Equivalent sound pressure level (dB) of the diverging orifice tube

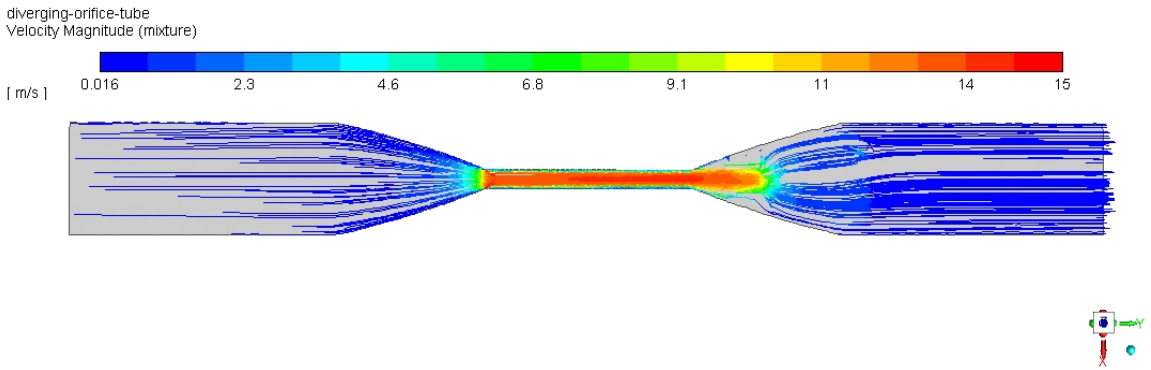

Figure 10: Velocity distribution of flow inside the parallel orifice tube

a. **b.**

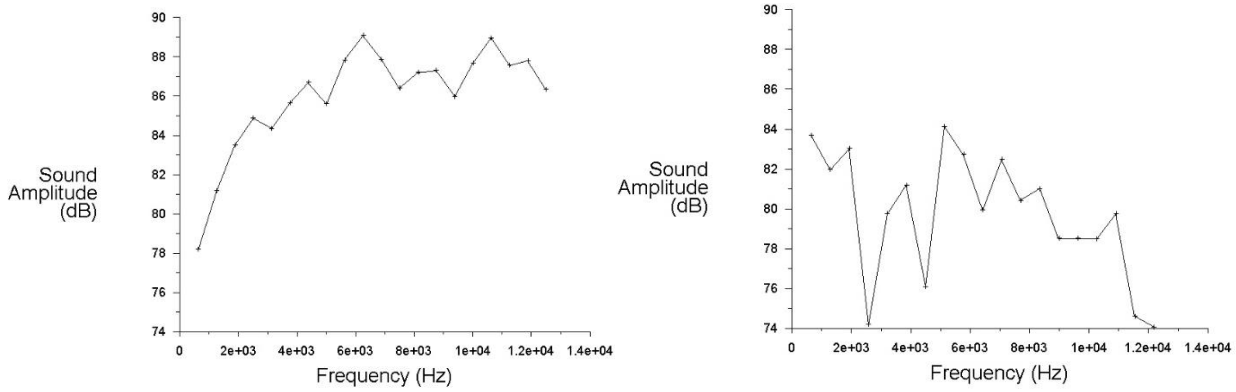

Figure 11: Flow-induced noise spectra for the parallel orifice tube (Fig 11a) and the diverging orifice tube (Fig 11b)

3.3 Acoustic Modelling Results of Orifice Tube with Different Tube Wall Thickness

Acoustic energy transmitted to the wall make the orifice tube vibrate with lower amplitude when increasing the tube wall thickness from 1 mm to 2 mm (as shown in Figure 12). The flow field inside the orifice tube is almost the same with that of 1 mm wall thickness. However, the amplitude of noise received by the receiver is smaller with 2mm-thickness orifice tube, especially in the high-frequency region (above 4 kHz). The vortex shedding frequency is between 3 kHz to 4 kHz and the flow oscillation induced by vortices will not couple with structure vibration. It seems reasonable that the vortex shedding noise only has slight change with different thicknesses of the wall (as shown in

Figure 13). The mitigation of noise through the increase of the tube wall thickness is more effective for high-frequency flow-induced noise.

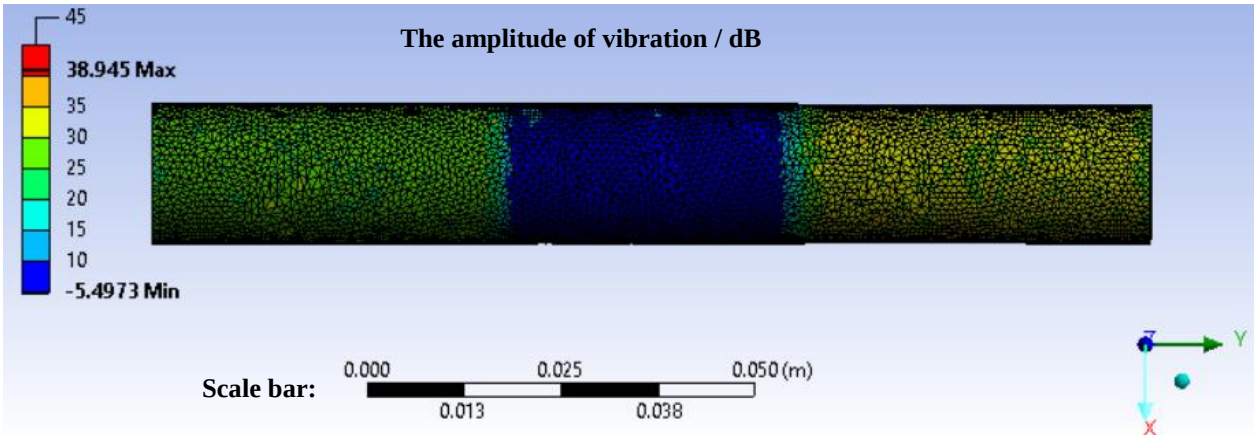

Figure 12: Equivalent sound pressure level (dB) of the 2mm-thickness parallel orifice tube

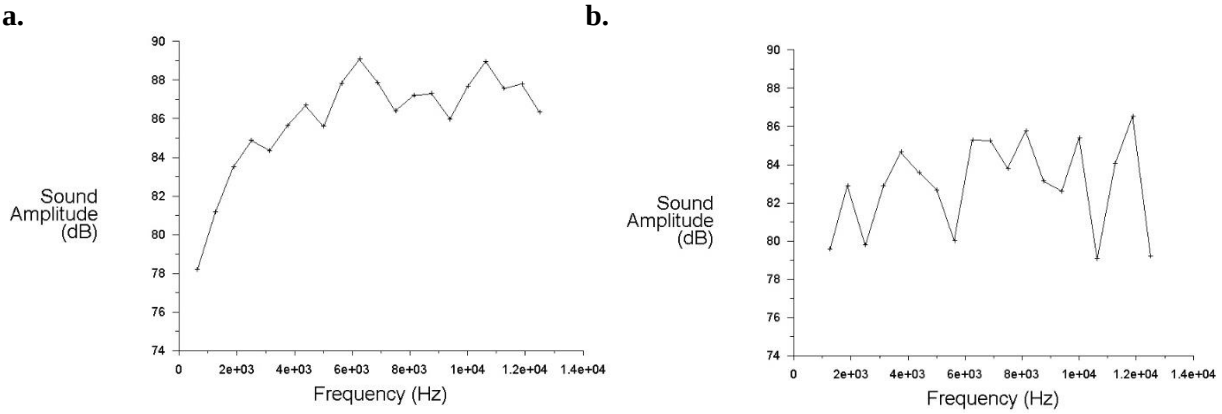

Figure 13: The flow-induced noise spectra for the parallel orifice tube with 1 mm-thickness (Fig 13a) and the parallel orifice tube with 2 mm-thickness (Fig 13b)

The thicker orifice tube starts vibrating at 8.7 kHz, whose lock-in range is from 7 kHz to 10.5 kHz. Similarly, the second order of the structural mode starts from 13.2 kHz, whose lock-in range is between 10.6 kHz to 15.9 kHz. The flow oscillation over 7 kHz can therefore vibrate in resonance with the structure. However, since the tube vibrates at a smaller amplitude, the coupled flow-induced noise decreases as well.

4. CONCLUSIONS

In this paper, a CFD based model is used to explore the geometry optimization of orifice tube using R134a. The model computes the interaction between the flow field and the structure with FSI model. The cavitation model with constant vapor pressure resolves the phase change when the fluid is passing through the orifice tube. For bulk fluid flow field, the LES turbulence model computes the fluid region successfully. In the coupling system, the results calculated by fluid model and structure model communicate with the interactive surfaces. The results show that changing the internal geometry from parallel structure to diverging structure mitigates the flow oscillations over the entire frequency domain. The flow regimes after being throttled by the constrained section determine the flow-induced noise. The possible noise sources include vortices, flashing flow, and collisions of fluid molecules with the solid wall. By increasing the thickness of the tube wall, the amplitude of the flow-induced is smaller than that with a thinner wall. A more massive tube wall attenuates the vibrating scope of the orifice tube, which weakens the resonance between the tube wall and flow oscillation. Modifying the internal geometry can mitigate the flow-induced noise more effectively, however, it may be costlier than adding tube wall thickness. The results are references for geometry optimizations of

other expansion devices, such as manual expansion valve and TXV. The results are reliable for that they match the previous theories well. Nevertheless, the modeling results stated in this paper need further testing with experiments.

NOMENCLATURE

Symbols and Abbreviations

a	tube radius	(m)
B	equivalent diameter of the bluff	(m)
d	internal diameter of the orifice tube	(m)
D	outer diameter of the orifice tube	(m)
E	modulus of elasticity	(N/m^2)
F	frequency	(Hz)
h	tube thickness	(m)
I	area moment of inertia	(m^4)
K	foundation stiffness	(N/m)
l	length of the tube	(m)
St	Strouhal number	(–)
v	Poisson's ratio	(–)
ρ	density	(kg/m^3)
λ	dimensionless parameter associated with a Particular structural natural frequency	(–)

Subscript

ma	material
mi	medium
m	axial mode shape number
n	circumferential mode shape number

REFERENCES

Blevins, R. D. (1979). *Formulas for Natural Frequency and Mode Shape*. New York: Van Nostrand Reinhold Co.

Blevins, R. D., & Bressler, M. M. (1993). Experiments on Acoustic Resonance in Heat Exchanger Tube Bundles. *Journal of Sound and Vibration*, 164(3), 503–533.

Chae, H. B., James W. S., & Michael R. M. (1990). Surface Tension of Refrigerants R123 and R134a. *Journal of Chemical and Engineering Data*, 35(1), 6–8.

Gijrath, H., & Ăbom, M. (2003). Flow Induced Noise Modelling for Industrial Piping Systems. *Proceedings of the Tenth International Congress on Sound and Vibration*, no.1, 1–8.

Jacob, M. C., Boudet, J., Casalino, D., & Michard, M. (2005). A Rod-Airfoil Experiment as a Benchmark for Broadband Noise Modeling. *Theoretical and Computational Fluid Dynamics*, 19(3), 171–96.

Lotfi, B., Bengt, S., & Wang, Q.W. (2016). 3D Fluid-Structure Interaction (FSI) Simulation of New Type Vortex Generators in Smooth Wavy Fin-and-Elliptical Tube Heat Exchanger. *Engineering Computations*, 33(8), 2504–29.

Mendez, S., Shoeybi, M., Lele, S. K., & Moin, P. (2013). On the Use of the Ffowcs Williams-Hawkings Equation to Predict Far-Field Jet Noise from Large-Eddy Simulations. *International Journal of Aeroacoustics*. 12(1–2), 1–20.

Rodarte, E., Singh, G., Miller, N., & Hrnjak, P. (1999). Refrigerant Expansion Noise Propagation Through Downstream Tube Walls. *SAE Technical Paper*.

Valipour R., Yeganeh B. A., Ghaheri A., & Kazeminezhad M. H. (2008). Determination of Vortex Shedding Frequency Around Offshore Pipeline Using Unsteady Drag Force Model. ASME. *International Conference on Offshore Mechanics and Arctic Engineering*. Volume 5: Materials Technology; CFD and VIV: 613-621.

ACKNOWLEDGEMENT

The authors would like to thank the member companies of the Air Conditioning and Refrigeration Center at the University of Illinois at Urbana-Champaign for their support.